Optical and transport properties of an alkali-doped methanofullerene

Saab, A. P.; Stucky, G. D.; Srdanov, V. I.; Hummelen, J. C.; González, M.; Wudl, F.

Published in:
Journal of Chemical Physics

DOI:
10.1063/1.1506146

Publication date:
2002

Optical and transport properties of an alkali-doped methanofullerene

A. P. Saab,[a] G. D. Stucky, and V. I. Srdanov[b]
Department of Chemistry and Biochemistry, University of California, Santa Barbara, California 93106

J. C. Hummelen,[c] M. González,[d] and F. Wudl[d]
The Institute for Polymers and Organic Solids, University of California, Santa Barbara, California 93106

(Received 22 January 2002; accepted 18 July 2002)

We examine the effects of monoderivatization on the electronic properties of C_{60}. For this we chose the phenyl-C_{61}-octanoic acid cholesteryl ester, [6,6]PCOCr, whose nonlinear optical properties have been investigated in the past. While the optical absorption spectrum of this methano fullerene is similar to that of C_{60}, substantial differences are observed upon doping with potassium. Similarly, the doping-dependent conductivity of the functionalized fullerene shows two maxima as opposed to the single maximum for C_{60}. The experimental observations are consistent with the doping-induced degeneracy removal of the parent C_{60} LUMO (t_{1u}) orbital, which in potassium-doped methanofullerene splits into two components separated by about 0.5 eV. We provide experimental evidence that the doping of [6,6]PCOCr proceeds, as in C_{60}, with six consecutive reduction (electron transfer) steps, yielding K_6[6,6]PCOCr stoichiometry at the end. The transport in partially doped [6,6]PCOCr thin films occurs by thermally activated hopping of the charge carriers with activation energy $E_a \cong 0.25$ eV and hopping probability proportional to the number of unpaired electrons in the reduced molecule. © *2002 American Institute of Physics.*
[DOI: 10.1063/1.1506146]

While the optical properties of C_{60} have been extensively studied,[1] little is known about the optical and transport properties of derivatized fullerenes. Unlike pristine $C_{60,}$ its compounds tend to decompose during sublimation, thus preventing epitaxial growth of solvent-free thin films, the most suitable form for optical studies. Thin films from solutions of such compounds are also difficult to obtain since most of them have poor solubility. Notable exceptions are certain methanofullerenes, shown in Fig. 1, whose functional groups consist of a benzene ring and a cholesteryl group attached to the bridgehead 61st carbon atom.[2] Such derivatives are soluble in common organic solvents, giving rise to viscous solutions from which optical-quality thin films can be obtained by spin coating. As in the case of C_{60}, photo-induced charge transfer has been detected in conjugated polymers doped with methanofullerenes,[3] whereas the optical-limiting properties of methanofullerenes were found to be better than in C_{60} (Ref. 4).

C_{60} can be functionalized to form products in which a C–C double bond shared by two 6-membered carbon rings is converted to a single bond (i.e., a [6,6] derivative or methanofullerene).[5] In this case, the C_{60} icosahedral symmetry is lowered, and it is of interest to see how the eigenstates of the parent molecule and the molecule electron affinity are affected by such a perturbation. Theoretical calculations indicated[6] that the most profound effect on the electronic states is a degeneracy removal of the C_{60} LUMO, t_{1u} orbital. In this study, we focus on the phenyl-C_{61}-octanoic acid cholesteryl ester, abbreviated hereafter as [6,6]PCOCr. The material used was 100% pure methanofullerene monoadduct, as determined by high performance liquid chromatography (HPLC) and proton and ^{13}C-NMR (Ref. 2). We examine the effects of the functionalization by utilizing correlated *in situ* optical and conductivity measurements of alkali metal-doped thin films of the methanofullerene. Such measurements can be instrumental in identifying the origin of the interband transitions in fullerenes.[7,8]

The [6,6]PCOCr methanofullerene in Fig. 1 was spin-coated from toluene solution onto fused-silica substrates con-

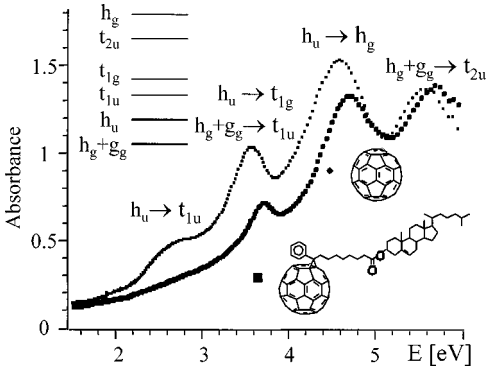

FIG. 1. Absorption spectra of pristine C_{60} (upper trace) and that of [6,6]PCOCr with the assignment of the most prominent electronic transitions in C_{60}. Of the two overlapping transitions at 3.6 eV, $h_g + g_g \rightarrow t_{1u}$ has a much higher oscillator strength (see Ref. 1 for details).

[a]Present address: Electronic and Electrochemical Materials and Devices, Los Alamos National Laboratory, Los Alamos, NM 87545.
[b]Author to whom correspondence should be addressed. Electronic address: srdanov@chem.ucsb.edu
[c]Present address: Department of Organic and Molecular Inorganic Chemistry, University of Gröningen, Nijenborgh 4, 9747 AG Gröningen, The Netherlands.
[d]Present address: Department of Chemistry and Biochemistry, Exotic Materials Institute, University of California, Los Angeles, CA 90095-1669.

taining two parallel gold pads separated by 3 mm. A thin film of pristine C_{60} was sublimed onto a separate substrate to a thickness of 80 nm, which roughly matched the optical density of the methanofullerene film. Absorption spectra in 1.5–6 eV region were recorded using a standard Hewlett-Packard 8452A diode-array spectrophotometer, whose optical cavity was modified in order to accommodate a remote vacuum chamber in its optical path.[7] The recorded energy range corresponds to the optical limit of the entire apparatus. The two substrates with films facing opposite directions were attached to a rod and sequentially exposed to potassium flux prior to spectral and conductivity measurements. Temperature-dependent conductance measurements were performed in an ultra-high vacuum chamber, equipped with a cold-finger cryostat. The methanofullerene sample was slowly doped at room temperature until a maximum or a minimum in conductance was reached, and then annealed at 400 K for 30 min. Temperature-dependent conductance measurements were made in 5 K increments beginning at 80 K, with the sample allowed to equilibrate for 10 min before each conductance value was recorded. The two-probe electric conductance was measured using a high input-impedance ($10^{12}\ \Omega$) meter, allowing for a lowest current reading of about 0.01 nS.

The optical absorption spectrum of pristine [6,6]PCOCr (Fig. 1) is strikingly similar to that of C_{60} above 3.0 eV except for a small but systematic 0.15 eV blue shift of the main spectral features. This shift can be linked to the loss of one π bond in [6,6]PCOCr, which lowers the C_{60} π-electron density by 3%. Notable differences occur in the optical absorption at the low energy where the parity-forbidden HOMO-LUMO ($h_u \rightarrow t_{1u}$) transition of C_{60} lies. The absorption of [6,6]PCOCr is distinctly weaker in this region, which may seem surprising considering that the symmetry reduction should eliminate the parity constraints. Breaking one fullerene double bond has apparently little effect on the symmetry of the molecular ground state electronic wave function, which still appears diagonal in the I_h representation. This is not the case with the vibrational spectra of monofunctionalized fullerenes, where changes due to functionalization are extensive. The optical spectrum of the methanofullerene is free from contributions from functional groups, such as ketone and phenyl groups, since their extinction coefficients[9] are two orders of magnitude lower than that of C_{60} (Ref. 10).

Doping with alkali metals transforms insulating C_{60} into a conductive ionic salt of the type K_xC_{60}, where $0<x<6$. Conductivity in K_xC_{60} is electronic because donated electrons occupy the three-fold degenerate t_{1u}-derived conduction band of C_{60} with itinerant electrons. The conductivity of K_xC_{60}, shown by an inset in Fig. 2, increases by several orders of magnitude with alkali doping, to reach 300 S cm^{-1} in K_3C_{60}, at which point the conduction band is half-filled with electrons.[11] Beyond this point, conductivity decreases monotonically to reach a minimum in the K_6C_{60} phase. Unlike C_{60}, the conductivity of potassium-doped [6,6]PCOCr shows *two conductivity maxima as a function of the dopant concentration.*[12] When exposed to a potassium flux, the conductivity of [6,6]PCOCr thin film increases steadily to reach a maximum of 0.1 S cm^{-1}, after which it decreases slowly to

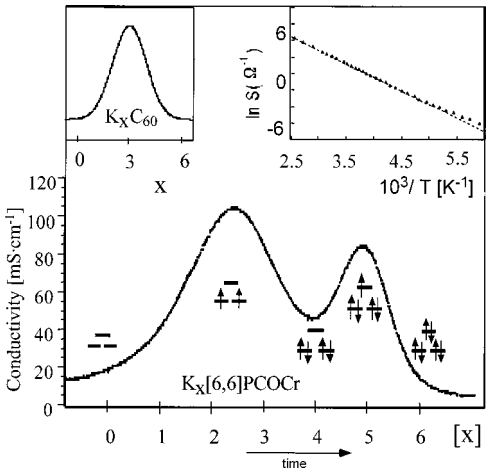

FIG. 2. Electrical DC conductivity of potassium-doped [6,6]PCOCr thin film as a function of the doping time. Suggested is the K_x[6,6]PCOCr stoichiometry as well as spin configuration of the localized electrons. Shown in the upper left corner are the conductivity measurements performed simultaneously on a thin film of C_{60}. Temperature-dependent conductance of the K_x[6,6]PCOCr stoichiometry that corresponds to the first maximum in conductivity is shown in the upper right corner.

a certain point where it starts to rise again. After the second maximum, conductivity decreases again to yield an insulating sample at the end of the doping cycle. The time required to complete doping of [6,6]PCOCr films was considerably longer than that of C_{60} due to the much slower diffusion of potassium ions through the amorphous solid. Systematic variation of the potassium flux showed that doping of C_{60} was limited by the potassium deposition rate, while potassium ion diffusion rate was the limiting factor in the case of [6,6]PCOCr. The diffusion constant of potassium ions in C_{60} is on the order of 10^{-16} m^2 S^{-1} (Ref. 13), while that of [6,6]PCOCr is about 30 times smaller. The conductivity of potassium-doped [6,6]PCOCr film is also lower than that of K_xC_{60} by about four orders of magnitude. The lower conductivity is in part due to the amorphous nature of the functionalized fullerene, which reduces mobility of the charge carriers.

The temperature-dependent conductivity of potassium-doped [6,6]PCOCr was measured at doping levels corresponding to the two maxima and two minima in the conductivity curve. The results for the first conductivity maxima are shown by the inset in Fig. 2. The temperature-activated hopping conductivity can be described by

$$\ln(s) = C - E/T^n, \tag{1}$$

where n is identically 1 for the nearest neighbor carrier hopping, C is a pre-exponential containing carrier attempt frequency, and E is the activation energy. The higher temperature region, for which $n=1$, was directly fitted to give the activation energies listed in Table I. The relatively large value of the activation energies arises from electron localization in the material, which in turn is due to considerable separation of the methanofullerene molecules caused by their long aliphatic tail. More importantly, however, we see that the activation energy for nearest-neighbor hopping is independent of the doping level and thus independent of the

TABLE I. Experimental activation energies, E_a, for different K_X[6,6]PCOCr stoichiometries.

X	2	4	5	6
E_a (eV)	0.25	0.25	0.22	0.25

fullerene oxidation state. Hence, based on the activation energies alone it would be difficult to reconcile the double maximum in the conductivity curve in Fig. 2, the degeneracy removal of the parent t_{1u} orbital therefore needs to be considered.

In $C_{60,}$ the t_{1u} LUMO is degenerate when either empty (C_{60}) or completely filled (K_6C_{60}) (Ref. 14). For the functionalized fullerene, theoretical calculations predict splitting of the three-fold degenerate parent t_{1u} orbital into a nearly doubly degenerate π-like orbital and a σ-like orbital, with a separation of about 0.4 eV (Ref. 6). The two conductivity maxima in Fig. 2 can now be explained assuming that the splitting between the two orbitals is larger than the corresponding electron correlation energy. Thus, K_4[6,6]PCOCr and K_6[6,6]PCOCr stoichiometries yield closed spin configurations, as indicated in Fig. 2, while K_1[6,6]PCOCr, K_2[6,6]PCOCr, K_3[6,6]PCOCr, and K_5[6,6]PCOCr consist of open-shell spin configurations which are held responsible for the conductivity observed in the experiment. Note that the ratio of the two conductivity maxima is 3:2 rather than 2:1, as it would be expected from the difference between the two stoichiometries with respect to the carrier density. We attribute this discrepancy to the slow potassium diffusion rate in amorphous [6,6]PCOCr, which makes it difficult to prepare homogeneous thin films of desired stoichiometry. Consistent with this is a residual conductivity at the K_4[6,6]PCOCr stoichiometry (the first conductance minimum during doping), which is probably due to the presence of methanofullerenes with open-shell configurations.

Owing to its molecular nature, the electronic orbitals in solid C_{60} can be assigned with the help of extended Hückel analysis of the isolated C_{60} molecule.[14] The same is true for alkali metal intercalated C_{60} (Refs. 1, 15), whose electronic transitions can be divided into two categories: the transitions originating from the C_{60} valence bands, consisting of h_u and (h_g+g_g) orbitals, and the transitions originating from the C_{60} t_{1u} conduction band. The first group persists in both pristine and alkali-doped fullerene with the exception of $h_g \rightarrow t_{1u}$ and $(h_g+g_g)\rightarrow t_{1u}$ transitions, which fade away once the t_{1u} orbital is filled. The second group of transitions, all originating from the t_{1u} orbital, is only present in doped phases. Wilson *et al.*[16] were the first to investigate changes in the absorption spectra of alkali-doped thin films of C_{60}, where the second group of transitions is clearly visible. Whereas Wilson *et al.* employed normalized differential absorption, $\Delta A_n=(A-A_o)/A_o$, we opt for simple differential absorption, $\Delta A=(A-A_o)$ in comparing absorption spectra of potassium-doped methanofullerene with those of C_{60}; in both cases, A_o and A represent absorbance of the undoped and doped fullerene, respectively. We choose simple differential absorption since normalized differential absorption tends to suppress changes in the high-optical density region

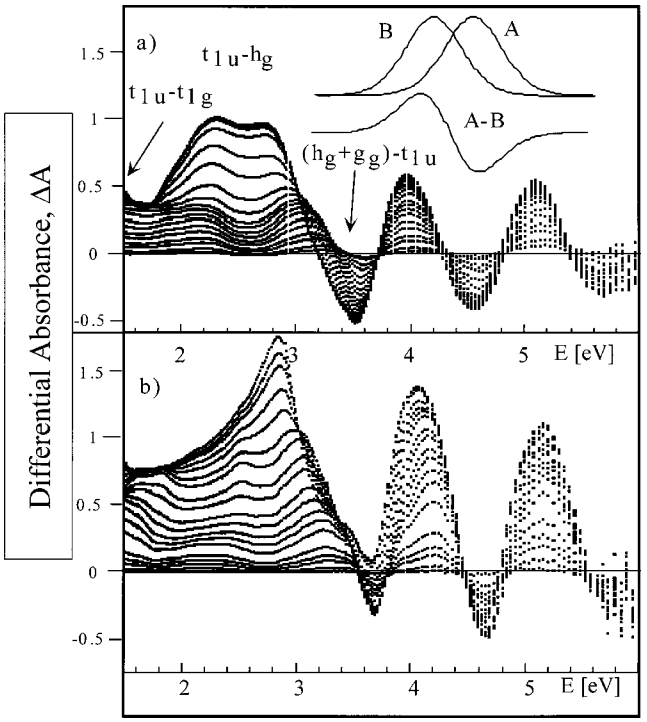

FIG. 3. Differential absorption spectra (ΔA) of potassium-doped thin films of C_{60} (a) and that of [6,6]PCOCr (b) taken in equal time intervals from the beginning to the end of the doping cycle. ΔA is zero everywhere at the beginning of the doping cycle and can increase or decrease in time. Positive ΔA normally indicates appearance of the new electronic transitions while negative ΔA indicates fading of the existing ones. Alternating negative/positive ΔA may indicate spectral shift of an absorption band, which leads to an oscillatory pattern clearly visible at the high-energy end of the spectra. Simulated by an inset is ΔA of the most prominent h_u-h_g transition of C_{60} at 4.5 eV (see Fig. 1), which is known to gradually shift towards 4 eV with potassium doping (Refs. 7 and 8). As a result, an oscillatory ΔA is obtained in agreement with experiment. The same applies to the rest of the absorption bands of C_{60}. Discussion regarding ΔA spectra of potassium-doped [6,6]PCOCr is given in the body of the article.

of the spectrum and, conversely, inflate the changes at the low-density end. For alkali-doped C_{60}, positive ΔA can imply transitions originating from the t_{1u} orbital, while negative ΔA suggests transitions terminating at that orbital. The changes in ΔA can also occur with shifting of the energy levels which, as we discuss below, complicates interpretation of the spectra.

In Fig. 3, ΔA of potassium-doped C_{60} in the 1.5–6 eV region is compared with that of potassium-doped [6,6]PCOCr. The absorption spectra were recorded every two minutes during alkali doping, but only a selected number of traces, separated by equal time intervals, is shown for clarity. Among the second group of transitions in potassium-doped C_{60}, only the $t_{1u}\rightarrow t_{1g}$ transition at 1.1 eV and the $t_{1u}\rightarrow h_g$ transition at 2.8 eV have been assigned with certainty.[1] Consistent with this is the positive ΔA in the low-energy region in Fig. 3(a) showing a shoulder at 1.5 eV (due to the $t_{1u}\rightarrow h_g$ transition at 1.1 eV) and a broad feature at 2.8 eV. The positive ΔA at 2.2 eV has been attributed previously to the $t_{1u}\rightarrow h_g$ vibrational sidebands.[16] Alternatively, this band may be the consequence of doping-induced splitting of the upper h_g band, visible in the density of states diagram of the alkali metal doped phases.[14] The C_{60} spectra in the 3.5–6 eV re-

gion in Fig. 3(a) contain alternating intervals of negative and positive ΔA. The negative ΔA at 3.6 eV is mainly due to bleaching of the $(h_g+g_g)\rightarrow t_{1u}$ transition with alkali doping, caused by the filling of the t_{1u} orbital with electrons. Once the t_{1u} is completely filled (as in K_6C_{60}), this transition ceases to exist. The same should happen to the parity-forbidden $h_u\rightarrow t_{1u}$ transition in C_{60} at 2.7 eV, but the negative ΔA in this region is outweighed by much stronger positive ΔA due to the $t_{1u}\rightarrow h_g$ transition. Besides $(h_g+g_g)\rightarrow t_{1u}$ and $h_u\rightarrow t_{1u}$ transitions, no other transitions in C_{60} are expected to terminate with t_{1u} orbital. Consequently, the experimentally observed negative ΔA at 4.5 and 5.5 eV in Fig. 3 cannot be explained by the same mechanism. Indeed, the change in ΔA observed for both C_{60} and [6,6]PCOCr can also be caused by spectral shifts of the electronic transitions that occur during alkali doping. As shown in the inset of Fig. 3, the oscillatory ΔA behavior can be simulated by a 0.5 eV bathochromic shift (shift towards lower energies) of a Gaussian peak with 0.8 eV half-width. The simulation is meant to mimic ΔA behavior of the first group of electronic transitions in C_{60}, which undergo a bathochromic shift during alkali doping.[7,8] This shift is particularly noticeable for $h_u\rightarrow h_g$ and $(h_g+g_g)\rightarrow t_{2u}$ transitions and is attributed to the structural transformations of the intercalated fullerene lattice.[16] The fact that such shifts also occur in the amorphous methanofullerene casts some doubts on the proposed origin of the shift, however. Instead, one can argue that adding electrons to the molecule increases screening of the Coulomb interaction between electron–hole pairs. This would produce a red shift of the electronic transitions, the magnitude of which should increase with the number of donated electrons.

Although ΔA spectra of potassium-doped [6,6]PCOCr in Fig. 3(b) show similar features to those of alkali-doped C_{60}, some important differences are present. At the low-energy end, a spectral feature appears at about 1.2 eV (when extrapolated to the beginning of the doping cycle), which gradually gains in intensity with doping and shifts towards 1.8 eV. This spectral feature stops to grow at about 2/3 of the doping cycle as if it originated from the lower (two-fold degenerate) component of the parent t_{1u} orbital. This feature, completely absent in Fig. 3(a), is highly consistent with 0.5 eV proposed splitting of the parent t_{1u} orbital. The two bands in the 2–3.5 eV region are also visible in Fig. 3(b), but their peak energies and relative intensities are slightly different from those in Fig. 3(a), as one may expect from two different molecules. The oscillatory behavior of ΔA above 3.5 eV is present in both spectra [Figs. 3(a) and 3(b)], yet ΔA is almost symmetric about $\Delta A=0$ in Fig. 3(a) and quite asymmetric in Fig. 3(b). A plausible explanation is that, besides the doping-induced spectral shifts that occur in both molecules, the two main absorption bands of potassium-doped [6,6]PCOCr in the near UV region gain an additional oscillator strength in the second half of the doping cycle. It is also possible that new electronic transitions that are parity forbidden in centrosymmetric C_{60} gain oscillator strength in noncentrosymmetric [6,6]PCOCr upon doping with potassium. Finally we note that spectra in Figs. 3(a) and 3(b) were both taken until no further changes in ΔA occurred, yet it appears as if some of the spectral features in Fig. 3(b) do not saturate. This only indicates that doping-induced spectral changes in certain parts of the spectra became accelerated towards the end of the doping cycle. More in-depth analysis of the observed electronic transitions in potassium-doped [6,6]PCOCr would require a detailed knowledge of the electronic states involved, as well as extensive near IR data.

In summary, the obvious similarity between absorption spectra of alkali-doped fullerene and methanofullerene argues on its own that, as in C_{60}, doping of the methanofullerene proceeds with six consecutive electron transfer steps, yielding K_6[6,6]PCOCr stoichiometry at the end of the doping cycle. Despite their lower strain energy,[17] methanofullerenes can be easily reduced, as demonstrated by cyclic voltammetry experiments.[18] Both transport and spectroscopy measurements of potassium-doped methanofullerene are consistent with the splitting of the parent t_{1u} orbital whose magnitude increases with doping. Due to its amorphous nature, conductivity in alkali-doped methanofullerene proceeds by thermally activated hopping.

[1] M. S. Dresselhaus, G. Dresselhaus, A. M. Rao, and P. C. Eklund, Synth. Met. **78**, 313 (1996), and references therein.
[2] J. C. Hummelen *et al.*, J. Org. Chem. **60**, 532 (1995).
[3] R. A. J. Janssen *et al.*, J. Chem. Phys. **103**, 788 (1995); M. Cha, N. S. Sariciftci, A. J. Heeger, J. C. Hummelen, and F. Wudl, Appl. Phys. Lett. **67**, 3850 (1995); K. Lee *et al.*, Phys. Rev. B **54**, 10525 (1996).
[4] L. Smilowitz *et al.*, Opt. Lett. **21**, 922 (1996).
[5] T. Suzuki, Q. Li, K. C. Khemani, F. Wudl, and O. Almarsson, Acc. Chem. Res. **25**, 157 (1992).
[6] Wanda Andreoni (unpublished work). See also Ref. 12 for more information regarding the predicted splitting.
[7] V. I. Srdanov *et al.*, Chem. Phys. Lett. **192**, 243 (1992).
[8] T. Pichler, M. Matus, J. Kurti, and H. Kuzmany, Solid State Commun. **81**, 859 (1992).
[9] R. M. Silverstein, G. C. Bassler, and T. C. Morrill, *Spectrometric Identification of Organic Compounds*, 5th ed. (Wiley, New York, 1991).
[10] A. F. Hebard, R. C. Haddon, R. M. Fleming, and A. R. Kortan, Appl. Phys. Lett. **59**, 2109 (1991).
[11] R. C. Haddon *et al.*, Chem. Phys. Lett. **218**, 100 (1994).
[12] F. Wudl, J. C. Hummelen, and V. I. Srdanov, *The Chemical Physics of Fullerenes 10 (and 5) Years Later: The Far-Reaching Impact of the Discovery of C_{60}*, edited by D. Wanda Andreoni, NATO Advanced Research Workshop on the Chemical Physics of Fullerenes 10 (and 5) Years Later (Kluwer Academic, Boston, 1996).
[13] G. P. Kochanski, A. F. Hebard, R. C. Haddon, and A. T. Fiory, Science **255**, 184 (1992).
[14] R. C. Haddon, Acc. Chem. Res. **25**, 127 (1992).
[15] V. I. Srdanov, C. H. Lee, and N. S. Sariciftci, Thin Solid Films **257**, 233 (1995).
[16] W. L. Wilson, A. F. Hebard, L. R. Narasimhan, and R. C. Haddon, Phys. Rev. B **48**, 2738 (1993).
[17] R. C. Haddon and K. Raghavachari, Tetrahedron **52**, 5207 (1996).
[18] M. Keshavarzk, B. Knight, R. C. Haddon, and F. Wudl, Tetrahedron **52**, 5149 (1996).